Supplementary data

Synthesis of Fe_3O_4@SiO_2 magnetic composites

Briefly, 1.35 g $FeCl_3$•$6H_2O$ was dissolved in 40 mL ethylene glycol to form an orange solution, then 2.05 g NaAc•$3H_2O$ was added. The mixture was stirred until the reactant were completely dissolved. After that, the mixture was transferred into a Teflon-lined autoclave with capacity of 50 mL and heated at 180 °C for 18 h. The products (Fe_3O_4) were naturally cooled down to room temperature and respectively washed with ultrapure water and ethanol for several times, which was then dispersed in ethanol for further use. 6 mL Fe_3O_4 magnetic fluid was added into three neck flask (250 mL), which was mixed with 6 mL ultrapure water and 30 mL ethanol. With the continuous mechanical agitation, 2 mL ammonia solution (25%) and 0.1 mL tetraethyl orthosilicate (TEOS) were consecutively added to the magnetic fluid mixture. This reaction was running at room temperature for 4 h under continuous mechanical agitation. After that, the resulting samples (magnetic separation) were washed by ultrapure water for three times. And then the samples were naturally (25 °C) dried overnight to obtain Fe_3O_4@SiO_2 magnetic composites.

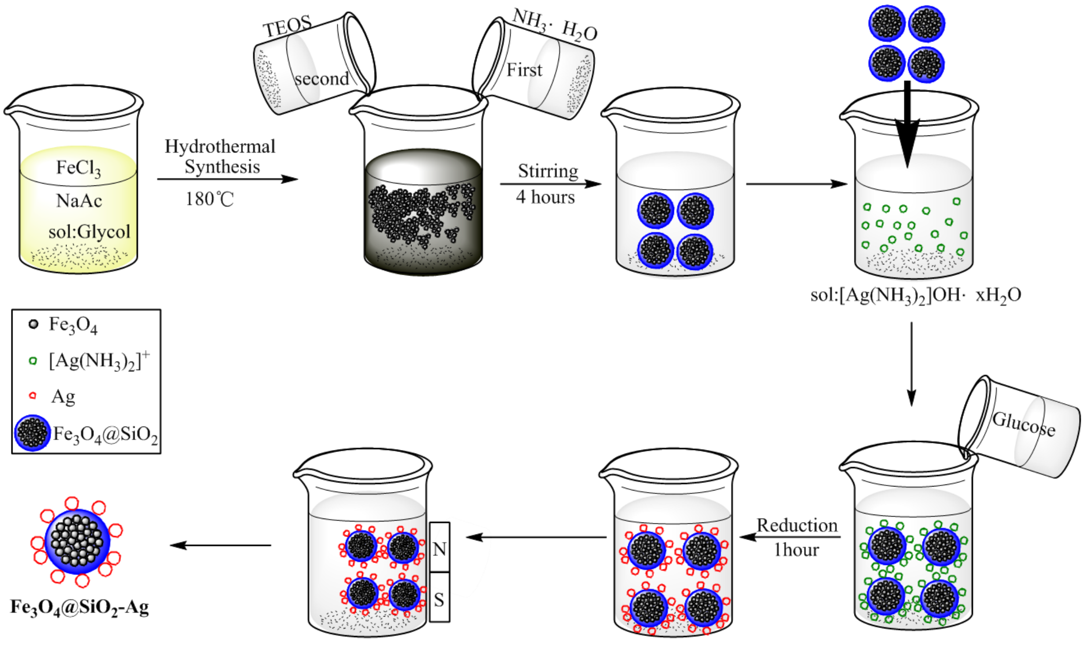

Figure S1 Synthesis route of MCMs-Ag.

Effect of synthesis conditions ($AgNO_3$ dosage, reaction time, and reaction temperature) on the antibacterial performance

The antibacterial performance of the MCMs-Ag is shown in Fig. S2, from which it can be seen that when $AgNO_3$ dosage is 80 mg, the remaining bacterial colonies are the least. When $AgNO_3$ dosage is below 80 mg, the antibacterial capacity of MCMs-Ag becomes stronger as $AgNO_3$ dosage increases. In contrast, when $AgNO_3$ dosage is above 80 mg, the antibacterial capacity of MCMs-Ag become weaker as $AgNO_3$ dosage increases. However, with the lower $AgNO_3$ dosage, a much stronger antibacterial capacity is observed than that with higher ones. It can be seen from Fig. S3a, b and c that the surface of MCMs-Ag is relatively smooth and no AgNPs is on it. As shown in Fig. S3d, the AgNPs are uniformly dispersed on the surface of the MCMs-Ag. Compared with Fig. S3e, Fig. S3f shows that AgNPs on the surface of MCMs-Ag have already begun to agglomerate. In Fig. S3f, some big aggregates are formed due to the serious aggregation of the AgNPs. The results indicate that the dispersity of the AgNPs on surface of MCMs-Ag with $AgNO_3$ dosage of 170 and 340 mg is worse than that with 80 mg. By analyzing the phenomena in Fig. S2 and Fig. S3, it is deduced that the MCMs-Ag with higher Ag-content have lower exposed AgNPs specific surface area and less released Ag^+ concentration, exhibiting lower antibacterial activity than that with lower Ag-content.[1] Therefore, by controlling the Ag-content (i.e. $AgNO_3$ dosage) on the surface of Fe_3O_4@SiO_2 magnetic composites, the antibacterial activity can be also controlled.

The antibacterial performance of MCMs-Ag with different reaction time is shown in Fig. S4, from which it can be seen that when reaction time is 120 min, the remaining bacterial colonies on the plate are the least. When reaction time is more than 120 min, the antibacterial capacity of MCMs-Ag has no obvious change compared with that of 120 min. In contrast, when reaction time is less than 120 min, the antibacterial capacity of MCMs-Ag is lower than that of 120 min. SEM images of the MCMs-Ag obtained with different reaction time are shown in Fig. S5. It can be seen from Fig. S5a, b and c that less AgNPs are present on the surface of MCMs-Ag. Fig.S5d shows that more AgNPs are attached on the surface of MCMs-Ag, but their sizes are very uneven. In Fig. S5e and f, the dispersity of the AgNPs on surface of MCMs-Ag is uniform and their sizes keep consistency. Besides, the size of as-obtained AgNPs in Fig. S5f is slightly larger than that in Fig. S5e. Thus, the size of AgNPs becomes relatively uniform as reaction time increases. In Fig. S5e, the AgNPs with uniform size and dispersity has larger surface area than others, which is propitious to contact with the bacteria completely. The result in Fig.S4 is consistent with the analysis of the SEM images.

The antibacterial performance of MCMs-Ag with different reaction temperature is shown in Fig. S6, from which it can be seen that when reaction temperature is 50 °C, there is no bacterial colonies remained in the water. The antibacterial capacity of MCMs-Ag with reaction temperature of 70 °C is as good as that with 50 °C. However, when reaction temperature is below 50 °C, the antibacterial capacity of MCMs-Ag is not as good as that of 50 °C. SEM images of MCMs-Ag with different reaction temperature are shown in Fig. S7. It can be seen that AgNPs are uniformly dispersed on the surface of MCMs-Ag and their sizes decrease as the temperature increases. As reported in previous study, AgNPs have a tendency for self-catalytic growth at higher temperature and the growth rate is fast,[2,3] so that the sizes of AgNPs are smaller. These results indicate that antibacterial capacity of smaller AgNPs is higher than larger ones, which is consistent with the results reported by others.[4] In summary, the optimal synthesis conditions for MCMs-Ag can be concluded as follows: 80 mg of $AgNO_3$ dosage, 120 min of reaction time and 50 °C of reaction temperature. Therefore, the following experiment are conducted with the optimal MCMs-Ag.

The EDX elemental analysis of samples synthesized under different conditions is shown in Table S1-Table S3, from which it can be seen that the amount of Fe, O, Si among samples are almost same, and the amount of Ag element is consistent with the analysis of the corresponding SEM images.

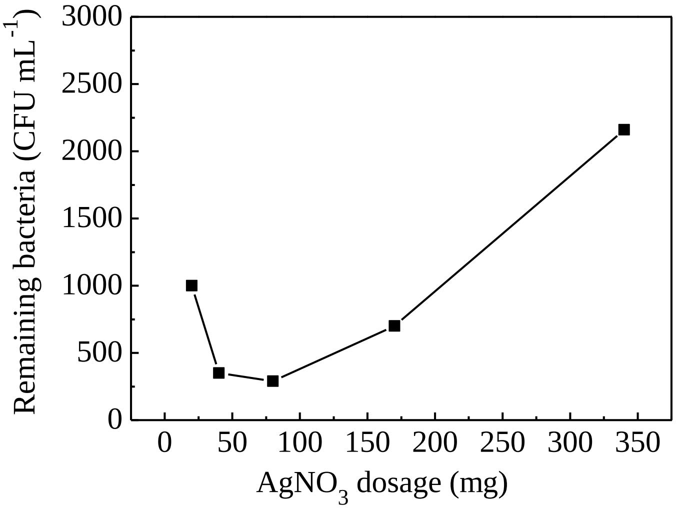

Figure S2 Effect of $AgNO_3$ dosage on antibacterial performance of MCMs-Ag.

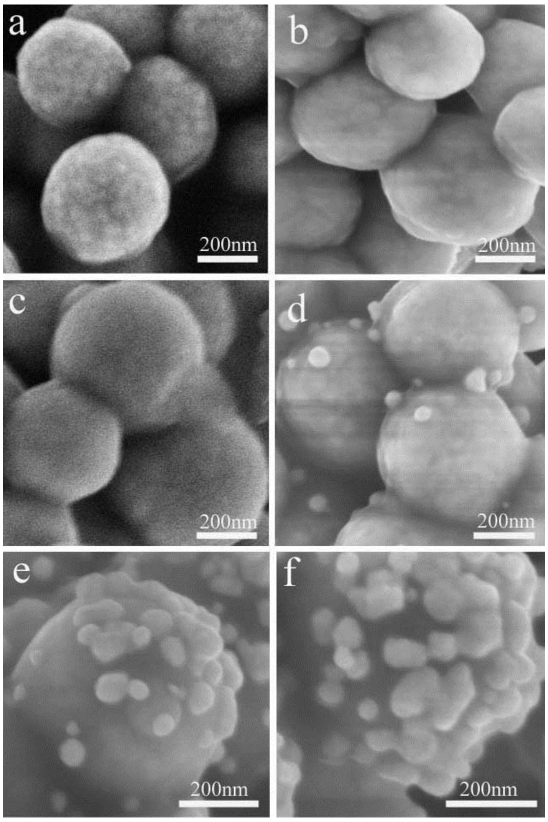

Figure S3 SEM images of MCMs-Ag with $AgNO_3$ dosage of (a) 0 mg, (b) 20 mg, (c) 40 mg, (d) 80 mg, (e) 170 mg, and (f) 340 mg.

Table S1 The EDX elemental analysis of of MCMs-Ag with different $AgNO_3$ dosage.

Conditions / Element(Wt%)	0.02 g	0.04 g	0.08 g	0.17 g	0.34 g
O K	15.50	14.15	14.81	12.97	15.23
Si K	17.62	17.97	12.34	18.03	15.54
Ag L	02.82	08.91	18.29	31.57	58.55
Fe K	61.06	62.89	51.27	60.71	50.68

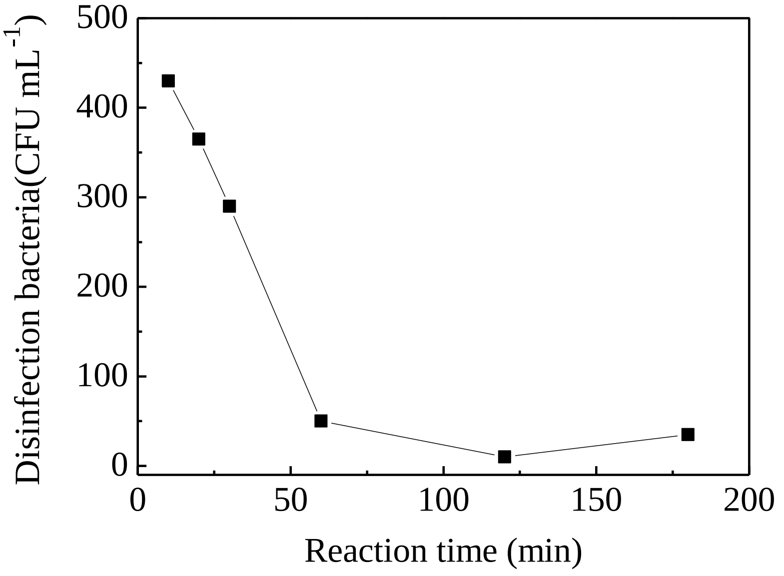

Figure S4 The antibacterial performance curve of MCMs-Ag with different reaction time.

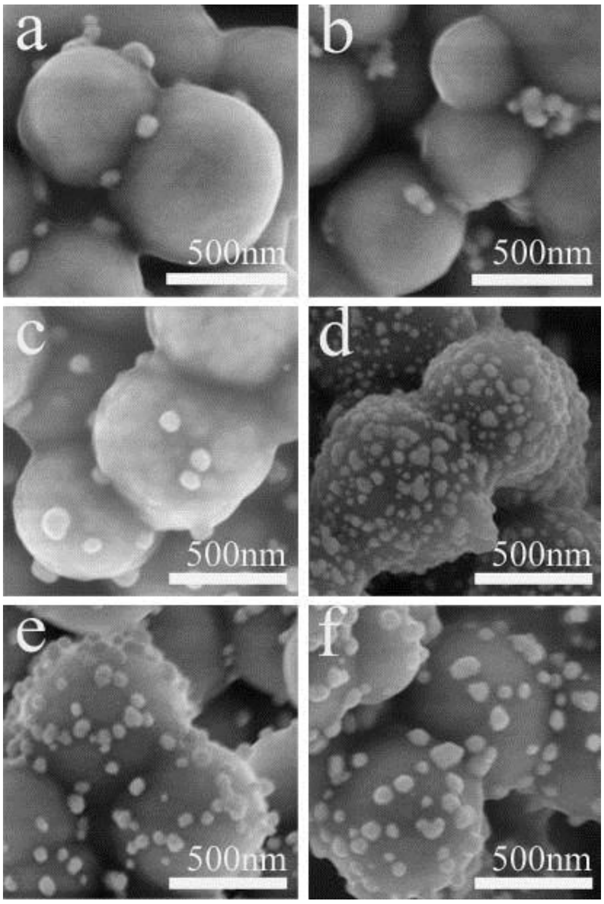

Figure S5 SEM images of MCMs-Ag with reaction time of (a) 10 min, (b) 20 min, (c) 30 min, (d) 60 min, (e) 120 min, and (f) 180 min.

Table S2 The EDX elemental analysis of of MCMs-Ag with different reaction time.

Conditions / Element(Wt%)	10 min	20 min	30 min	60 min	120 min	180 min
O K	11.34	12.32	12.45	13.88	15.59	15.93
Si K	14.31	14.72	14.49	14.26	15.11	17.90
Ag L	15.78	14.66	15.91	23.88	28.75	20.36
Fe K	48.56	44.30	48.32	47.98	50.55	55.80

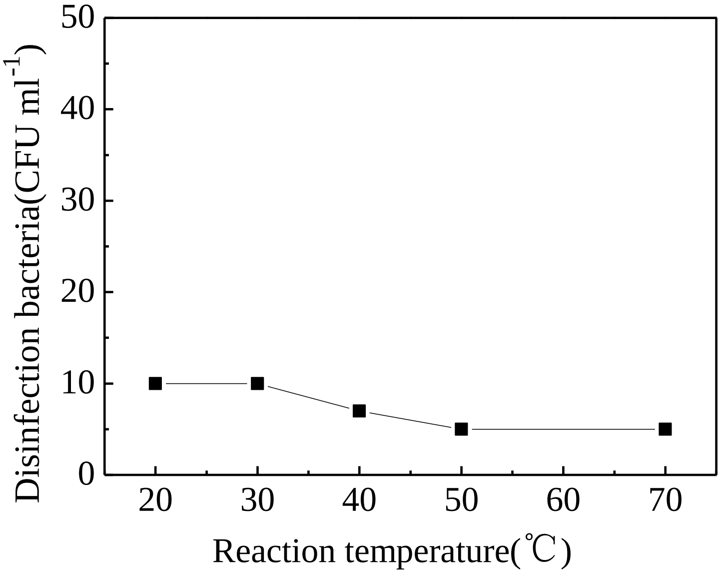

Figure S6 The antibacterial performance curve of MCMs-Ag with different reaction temperature.

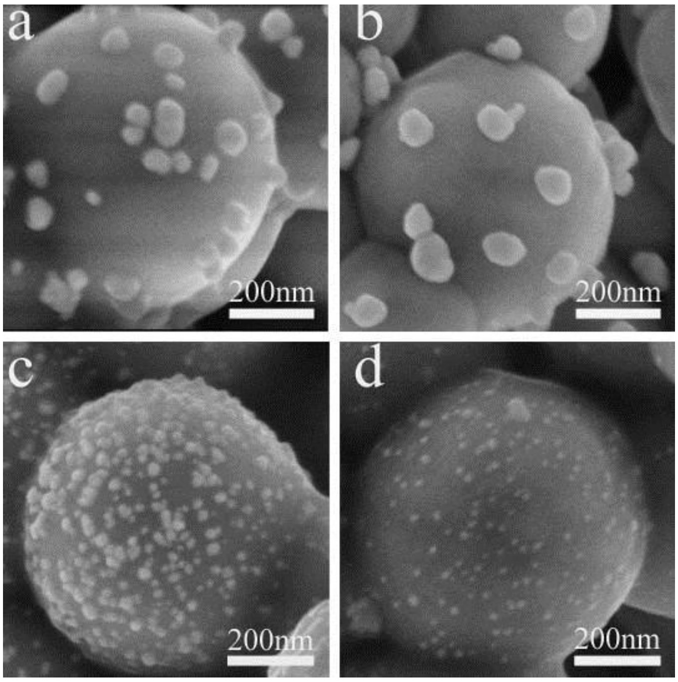

Figure S7 SEM images of MCMs-Ag with different reaction temperature (a) 25 °C, (b) 30 °C, (c) 50 °C, (d) 70 °C.

Table S3 The EDX elemental analysis of of MCMs-Ag with different reaction temperature**.**

Conditions / Element(Wt%)	25 °C	30 °C	40 °C	50 °C	70 °C
O K	12.87	12.96	11.13	12.32	14.78
Si K	15.66	14.56	15.27	12.40	11.21
Ag L	28.65	26.59	18.24	16.71	15.91
Fe K	45.33	46.15	51.37	58.57	41.44

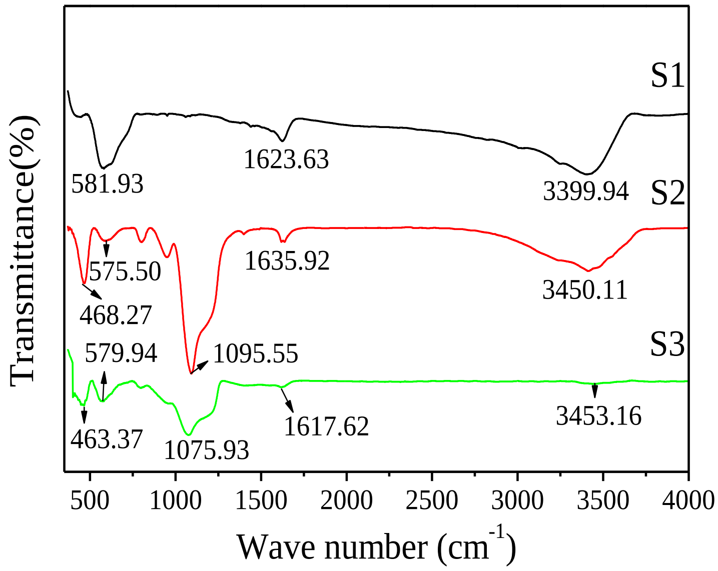

Figure S8 FT-IR spectra of MCMs-Ag (S1-Fe_3O_4, S2-Fe_3O_4@SiO_2 magnetic composites and S3-MCMs-Ag).

References

1. Y. H. Kim, C. W. Kim, H. G. Cha, D. K. Lee, B. K. Jo, G. W. Ahn, E. S. Hong, J. C. Kim and Y. S. Kang, *J. Phys. Chem. C*., 2009, **113**, 5105–5110.
2. C. Besson, E. E. Finney and R. G. Finke, *J. Am. Chem. Soc*., 2005, **127**, 8179−8184.
3. M. Han, S. L. Liu, X. P. Nie, D. Yuan, P. P. Sun, Z. H. Dai and J. C. Bao, *RSC Advances*., 2012, **2**, 6061–6067.
4. Y. H. Kim, D. K. Lee, H. G. Cha, C. W. Kim and Y. S. Kang, *J. Phys. Chem. C*., 2007, **111**, 3629–3635.